Empirically Derived Sensitivity of Vegetation to Climate Across the Globe

Gregory Ross Quetin

A thesis
submitted in partial fulfillment of the
requirements for the degree of

Master of Science

University of Washington

2015

Reading Committee:

Abigail L. S. Swann, Chair

David Battisti

Dennis Hartmann

Program Authorized to Offer Degree:
Atmospheric Sciences

University of Washington

Abstract

Empirically Derived Sensitivity of Vegetation
to Climate Across the Globe

Gregory Ross Quetin

Chair of the Supervisory Committee:
Assistant Professor Abigail L. S. Swann
Department of Atmospheric Sciences

To predict the response of vegetation to climate change, we must understand the physiological processes controlling productivity across large spatial scales, encompassing global climate space. To date there is not a fully empirical map of vegetation sensitivity to climate at the global scale. We use the response of satellite-based greenness (from Normalized Difference Vegetation Index) to inter-annual climate variations in surface air temperature (from ERA-Interim) and precipitation (from Global Precipitation Climatology Project) to derive the sensitivity of vegetation to temperature to infer mechanisms of climate constraint on vegetation productivity across the globe as represented by greenness. We focus on how the sensitivity of vegetation to temperature varies across climate space, finding that it is modulated by a balance of resources. The majority of grid cells in simultaneously warm (above 14 °C) and dry (below 1000 mm/year rainfall) conditions have negative vegetation sensitivity to temperature (browner in warm years) while at places with cooler temperatures the vegetation sensitivity is generally positive (greener in warm years). The mean annual temperature boundary between positive and negative sensitivities changes by 9 degrees C depending on how much rainfall a place receives. At very high rainfall levels (beyond 3000 mm/year), even the hottest vegetated places on Earth have positive sensitivity to mean annual temperature. The positive temperature sensitivity of these warm wet ecosystems suggests that water allows

buffering against damaging maximum temperatures and that these ecosystems may actually benefit from near term warming on the scale of inter-annual variations of temperature.

TABLE OF CONTENTS

LIST OF FIGURES

LIST OF TABLES

ACKNOWLEDGMENTS

Abigail Swann for her patient mentorship and support during this research. David Battisti and Dennis Hartmann for serving on my Master's committee and their numerous suggestions. Leander Love-Anderegg for multiple readings and discussions.

Chapter 1

INTRODUCTION

To date there is not a fully empirical map of climate constraints on vegetation at the global scale. We depend on observing where vegetation is currently and scaling up physiological models to understand global productivity. The productivity of vegetation across the world is coupled to the climate and controls the terrestrial carbon cycle [Friedlingstein et al. 2006], the terrestrial hydrological cycle [Schlesinger and Jasechko 2014] [Jasechko et al. 2013] and surface energy budget [Ghimire et al. 2014]. To predict the response of vegetation to climate change, we must understand the physiological processes controlling productivity at large spatial scales, and thus across global climate space. We can identify how processes are controlling productivity across these ranges by analyzing how vegetation productivity responds to variations in temperature, vapor pressure deficit and shortwave radiation over time.

Vegetation absorbs sunlight to fix carbon dioxide (CO_2) into sugars through photosynthesis. This CO_2 fixation is regulated by environmental conditions including local temperature and water availability through the moderation of activity in the Calvin-Benson Cycle, activation of Rubisco and other physiological processes [Eaton-Rye et al. 2011] pg.284-285 involved in plant growth. These environmental regulations on photosynthesis act at very local scales, from the scale of the whole plant down to that of the leaf or smaller. The global consequences of these local controls are usually studied by attributing climate classifications based on the distribution of vegetation biomes [Peel et al. 2007] [Kottek et al. 2006] [Smith et al. 2002] [Thornthwaite 1948] [Metzger et al. 2013], simplified models based on physiology [Nemani et al. 2003] or by extending plant or plot scale research to the global scale through Earth System Models that include the most detailed knowledge of physiology possible [Ole-

son et al. 2010]. This study takes a unique approach to classifying bioclimatic zones and climate constraints across the globe by using data on vegetation greenness to directly assess the underlying climatic constraints on plant productivity.

1.1 Climate Classification

Climate classification attempts can suggest hypotheses for the processes that determine each bioclimate zone but have no direct information to test the hypotheses. Climate classification approaches use the distribution of observed vegetation (i.e. Rainforest, Tundra) to define climate envelopes. Thresholds of mean annual temperature and precipitation along the boundary of a biome are used to classify the Earths surface into bioclimatic zones [Peel et al. 2007] [Kottek et al. 2006] [Smith et al. 2002] [Thornthwaite 1948]. The most modern and innovative climate classification techniques, though able to determine the climate variables that represent the majority of climate variance across the globe (growing degree days, aridity index, temperature seasonality and potential evapotranspiration seasonality), can only describe physical differences in biomes and are not able to determine the process by which the vegetation is constrained by environmental factors [Metzger et al. 2013]. By contrast, the analysis presented here directly observes constraints on vegetation using the NDVI (vegetation greenness) response to inter-annual variability of temperature.

1.2 Models of Global Climate Constraints on Vegetation

While climate classifications are unable to identify mechanisms and processes controlling vegetation productivity, at the other end of the spectrum a number of studies have created simple models inspired by plant physiology to map climate constraints on vegetation across the globe [Churkina and Running 1998] [Nemani et al. 2003] [Jolly et al. 2005] [Running et al. 2004] [BOISVENUE and RUNNING 2006]. In each case the maps were created using broad annual characteristics of climate such as mean annual temperature, growing season length, mean annual net surface shortwave radiation and mean annual atmospheric vapor pressure deficit to capture the climate constraints of temperature, water and energy on

vegetation. These models complement climate classification techniques by lending insight into the broader effect of mechanisms measured on a plant scale but are ultimately derived from plant scale studies, and so can not themselves be used to test process based models. Our analysis serves to combine aspects of both the climate classification and process based approach to provide an empirical distribution of climate constraint with the potential to test Earth System models. We present results for a fully empirical global map of climate constraints on vegetation, and differentiate between what climate factors of temperature, precipitation, shortwave radiation and vapor deficit drive the broad patterns.

1.3 History of Normalized Difference Vegetation Index (NDVI) and Climate

The nearly 30-year multispectral satellite record of NDVI represents the longest global time series available to study vegetation response at a scale commensurate with large fluxes of carbon and ecological-climate feedbacks [Pinzon and Tucker 2014]. NDVI has frequently been used to study temporal trends in vegetated land cover [Chen et al. 2014] and has been correlated with physical parameters across biomes and regions to demonstrate the connection between climate and vegetation [Zhou et al. 2003] [Zhou et al. 2001] [Goward et al. 1991]. For example, in the tropics NDVI correlates strongly with El Nino and the changes driven in temperature and precipitation [Asner et al. 2000][Xu et al. 2014] [Myneni et al. 2002]. We can use the response of NDVI to inter-annual climate variations to determine a vegetation sensitivity to climate variation at each grid cell. A positive regression between NDVI and climate shows positive vegetation sensitivity (i.e. greener in a warmer year) while negative regression shows negative vegetation sensitivity (i.e. greener in a cooler year).

1.4 Interpretation of an Ecosystem Performance Curve

We can apply the concept of a plant performance curve to our analysis of vegetation. Observing the sensitivity of vegetation to inter-annual variability in climate allows us to measure the average slope of the performance curve for a given set of climate conditions. If the sensitivity of vegetation to changes in temperature is close to zero, this indicates that the ecosystem

is in relative balance (i.e. adequate water for the temperatures it experiences). Assuming a shape for the general performance, the magnitude of the slope shows whether the ecosystem is in a state of strong or weak positive constraint (i.e. too cold) or negative constraint (i.e. too hot) (Figure 1.1). As a parallel, in amphibians studies (i.e. small ectotherms), the full shape of this curve can be determined for an individual species with laboratory experiments. Curves for different species of a similar type (e.g. amphibians) show a change in the broadness of the thermal tolerance range (width of the performance curve) across latitude, i.e. changes in mean climate state [Deutsch et al. 2008][Huey 1991]. Specifically, [Deutsch et al. 2008] show that species from the tropics, where both seasonal and inter-annual variability in climate is low, show a narrower range of tolerance compared with species from higher latitudes where climate is far more variable. Though we are unable to reconstruct the shape of the curve itself for vegetation, our sampling provides information to the general position of the ecosystem on the curve . The variation of vegetation sensitivity across multiple climatic variables reveals the actual climate constraint to be a balance of resources. For example, the vegetation in a cold place with ample water supply will be more positively sensitive to warming than a dry cold place where there are multiple climate constraints.

In this thesis we will first discuss the vegetation and climate data used in the analysis. Then we will layout out the methods used in calculating the vegetation response to inter-annual climate variability, and the binning technique we used to investigate the systematic variation of vegetation response across climate. The focus of the results of the analysis will be on the vegetation response to temperature. Finally, we will discuss the patterns of climatic constraints, how water and temperature both establish the vegetation response, the consequences for the response of vegetation to global warming and conclusions on the adaptations and tradeoffs inherent in maximizing performance at the ecosystem level for different climatic conditions.

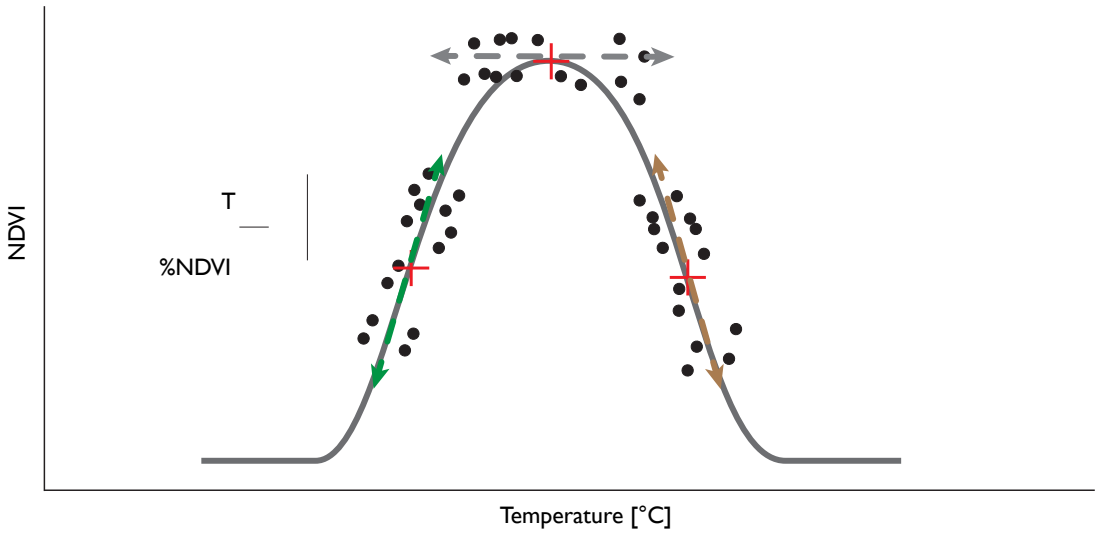

Figure 1.1: Schematic of how regression of temperature anomalies and NDVI anomalies sample the performance curve. Three possible outcomes [green] positive sensitivity, [grey] neutral, [brown] negative sensitivity.

Chapter 2

METHODS

2.1 Data Description

To investigate global patterns in vegetation responses to inter-annual climate variation, we combined surface greenness estimates from Normalized Difference Vegetation Index and the climate fields of temperature, precipitation, vapor pressure deficit and shortwave radiation to assess how the long-term mean climate defines vegetation responses to inter-annual climate variations. For example, we quantified how dry areas respond to increases in temperature compared to relatively wet areas. In the following section we introduce the datasets, time periods and resolutions used along with calculated metrics and climate variables.

2.2 Normalized Difference Vegetation Index

The NDVI 3g time series is an improved global Normalized Difference Vegetation Index dataset from the Advanced Very High Resolution Radiometers (AVHRR) [Pinzon and Tucker 2014]. NDVI is calculated by normalizing the difference between the visible channel and near-infrared channel from the AVHRR instruments by the sum of the channels. Vegetation absorbs strongly in the visible band, distinguishing it from soils and other surfaces. In this study we will interpret NDVI as a proxy for the surface greenness and chloroplast density to calculate the response of vegetation. Though not treated here, NDVI also relates to Leaf Area Index and Fraction of Absorbed Photosynthetically Active Radiation [Myneni et al. 2002]. The dataset has a 1/12-degree latitude-longitude resolution and global coverage of 15-day global maximum composites that we will aggregate to max monthly 1°x 1°resolution. The datasets processing into maximum composites reduce effects from cloud and satellite viewing angle [HOLBEN 1986].

Dataset	Measurement	Spatial Resolution	Time Resolution	First - Last Yr
NDVI 3g	NDVI	1/12 degree	Bimonthly	1982-2012
GPCP	Precipitation	1x1 degree	Daily	1996 - 2013
ERA-INTERIM	Temperature	1x1 degree	Monthly	1979-2013
ERA-INTERIM	Dew Point Temp	1x1 degree	Monthly	1979-2013
CERES-SYN	Radiation	1x1 degree	Monthly	2000-2013
SRB REL3.1	Radiation	1x1 degree	Monthly	1983-2007

Table 2.1: Summary of the data used in the analysis.

2.3 ERA-Interim Reanalysis

For surface temperature and dew point temperature (used in calculating vapor pressure deficit) we used two-meter ERA-Interim Reanalysis 1°x 1°latitude-longitude monthly global dataset covering 1979 - 2012 [Dee et al. 2011]. The two-meter data is closest to the surface climate experienced by the vegetation.

2.4 NASA/GEWEX SRB 3.1

For shortwave downward surface radiation climate calculations we used the Surface Radiation Budget 3.1 (SRB 3.1) 1°x 1°latitude-longitude monthly dataset available from 1983 to 2007 [NASA/GEWEX SRB 3.1 Data].

2.5 Global Precipitation Climatology Project

We calculated a monthly precipitation dataset by summing daily precipitation from the GPCP global dataset of 1°x 1°latitude-longitude available from 1996 to 2012 [Adler et al. 2003]. The GPCP dataset of precipitation is a combination of satellite and gauge data interpolated across the globe.

2.6 Calculated Vapor Pressure Deficit

2.6.1 Vapor Pressure Deficit

Vapor pressure deficit is a non-linear function of temperature and combines information about both the temperature and water content of the atmosphere. The vapor pressure deficit describes the difference between the partial pressure of water in the atmosphere and a fully saturated surface in the local conditions. We derived vapor pressure deficit and relative humidity using an empirical equation appropriate for atmospheric conditions [NOAA Approximation].

$$VPD = e_s - e$$

$$RH = \frac{e}{e_s}$$

$$e_s = 6.11 \times 10^{((7.5*T)/(237.3+T))}$$

$$e = 6.11 \times 10^{((7.5*Td)/(237.3+Td))}$$

Here the vapor pressure deficit (VPD) is the difference between the saturated vapor pressure (e_s) and the actual vapor pressure (e). We calculated the vapor pressures from the monthly temperature (T) and dew point (Td) using estimations by NOAA. The vapor pressure deficit can be calculated by combining temperature and dew point and serves as a metric for soil moisture [Duff et al. 1997]. In the Ball-Berry formulation of stomatal conductance the gradient between the fully saturated vegetation and the atmosphere is an important factor determining transpiration and water stress [Ball et al. 1987]. When the atmosphere is less than fully saturated it creates a gradient between the fully saturated vegetation cells and the atmosphere (similar to evaporation off of a liquid water surface). If this gradient is large enough, and local soils are dry enough it can cause water stress for

vegetation.

2.7 Data Processing to Matched Spatial and Temporal Grid

We linearly interpolated all the data to a common 1x1 latitude-longitude grid using Matlab interp2.m. To create a common time step we created monthly maximum composites from the NDVI 15-day composites. This compositing has the added benefit of further reducing impacts from clouds or satellite viewing angles.

2.8 Methods

In the following section we introduce the methods used to calculate the vegetation response to inter-annual climate variability using NDVI. Included in the section are descriptions of the global grid cells masked and not considered in the analysis, periods of time used for analysis, the regression of NDVI annual anomalies against climate annual anomalies, the binning of data across climate space and the statistical tests we performed.

2.9 Data Masks

Our analysis considered only vegetated terrestrial grid points. We removed ocean grid points using the water mask present in the NDVI 3g maps. Terrestrial grid cells with very low or no vegetation were removed using a modified NDVI threshold [Zhou et al. 2001]. We determined a grid cell to be non-vegetated pixel if the minimum of the three maximum NDVI values of each year was below .1 or the mean of the three maximum values was below .3. Grid points with data missing at any of the considered times in any of the datasets were also removed.

2.10 Data Overlap

For our analysis of vegetation sensitivity to temperature we used the longest overlap of NDVI, temperature and solar radiation at 1°x 1°resolution from 1984 - 2007 (24 years). To calculate the long term climates of each grid cell we used either the overlapping time series or the longest possible time series where an overlap was not available.

2.11 Calculating Vegetation Sensitivity to Inter-annual Climate Variability

We calculated the vegetation sensitivity to climate at each grid point by using a linear regression of the annual percent anomalies of NDVI against the annual anomalies of temperature, vapor pressure deficit and shortwave radiation. The resulting sensitivity is expressed in % NDVI change per unit climate variation (i.e %NDVI/°C), which we term the vegetation sensitivity to temperature (or vapor pressure deficit or shortwave radiation) inter-annual variation.

These vegetation sensitivities are calculated at each grid point for the overlapping time series as a way to quantify the vegetation sensitivity across space.

2.12 Binning Vegetation Response Across Climate Space

Across the globe many points share a similar climate characterized by similar temperature, insolation and precipitation. We classify vegetation sensitivity in climate space by grouping grid cells into bins with an equal percentage of points. For example, when binning along temperature we ordered the points from coldest places to warmest and defined each bin as containing 1% of the total points. We performed this same analysis on temperature, vapor pressure deficit, shortwave radiation and precipitation. To investigate the systematic variation of vegetation responses across the climate space we calculated means of the vegetation sensitivity in each bin. Before averaging each grid cell was weighted by the area of the grid cell and the uncertainty of the correlation between NDVI and climate scaled from 0 (50% chances) to 1 (100% confidence) at each grid cell. The binning technique is similar to the common practice in climate science of calculating the zonal mean of a variable, where here we replace latitude with a climate variable (ex: Temperature) to examine the mean structure of the vegetation sensitivity.

2.12.1 Binning in multiple dimensions

The same techniques as described above were used when we subdivided multivariate climate space (ex: mean Temperature and mean Precipitation), by sorting and binning each set in series. For example, after creating bins in temperature, inside each temperature bin, the data is binned again in precipitation.

2.12.2 Statistical Significance of Vegetation Sensitivity

For our analysis of the vegetation sensitivity of the globe we consider each grid cell in the bin as a unique measurement. The weighted composite mean of the vegetation sensitivity can be statistically tested against zero with a student t-test using the full degrees of freedom as represented by number of grid cells in the bin (n-1).

Chapter 3

RESULTS

Here we present the results from calculating vegetation sensitivity as observed with NDVI to the inter-annual variability of temperature. First we summarize the global distribution of the vegetation sensitivity to climate variables of temperature, vapor pressure deficit and shortwave radiation.Next we demonstrate the systematic variation of vegetation sensitivity to temperature as a function of mean climate. Finally we show how vegetation sensitivity and thus climate constraint vary across multiple climate dimensions. In a given location, we consider a positive response of vegetation to a climate anomaly to indicate that the ecosystem is constrained by having too little of a particular variable (ex. too cold or energy constrained), while we interpret a negative response as having too much (ex. too hot or too dry).

3.1 Global Sensitivity of Vegetation to Climate

The global distribution of the vegetation sensitivity to temperature has a broad, nearly Gaussian distribution (solid line, Figure 3.1)(Table 3.1) with a mean to the right of zero (0.68 %NDVI/°C). The area of the globe constrained by cold temperatures (positive vegetation sensitivity) is nearly twice that of the area constrained by overly warm temperatures.

In contrast to vegetation sensitivity to temperature, the sensitivity of vegetation to vapor pressure deficit (thick dashed line, Fig 3.1) shows a mean very close to zero (3.66 %NDVI/hPa) with a more peaked distribution (Figure 3.1)(Table 3.1). There is a longer tail for values of positive vegetation sensitivity to VPD that occur in places with generally low VPD, places that are cold or wet. The extended positive tail of the distribution is reminiscent of the skewed distribution of rainfall. Finally, the sensitivity of vegetation to shortwave radiation

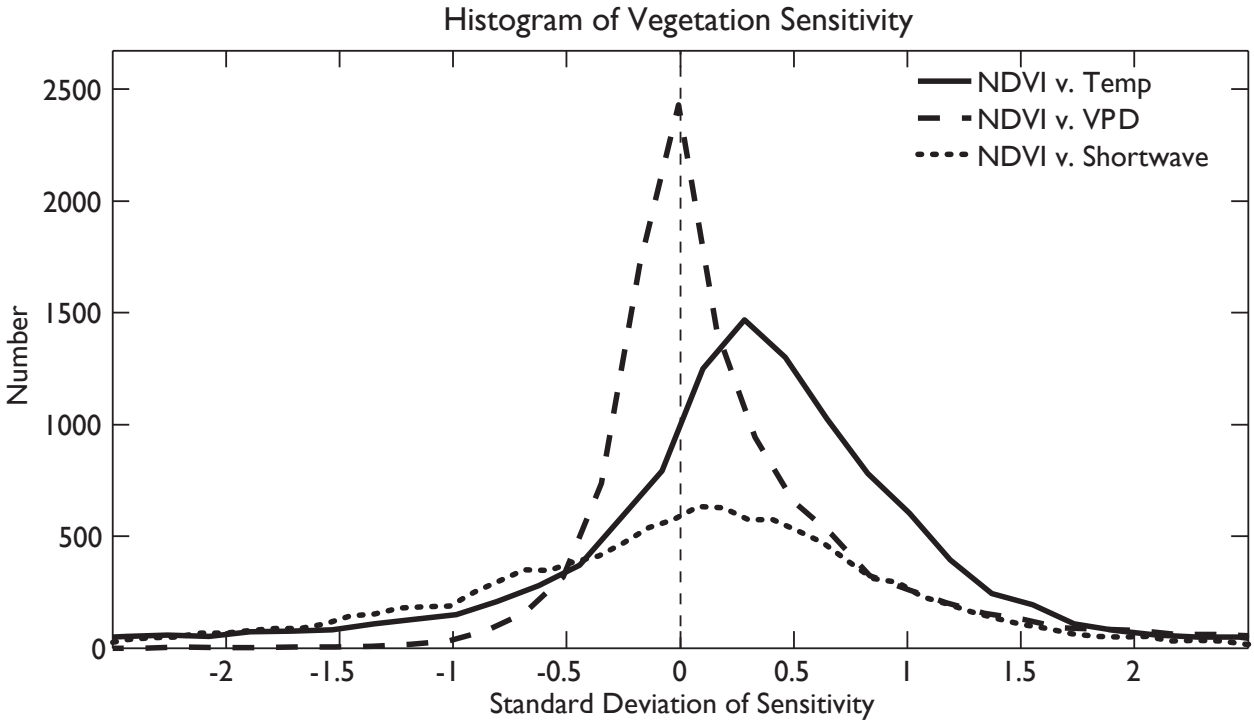

Figure 3.1: Histograms of the regression slope of annual anomalies in NDVI and temperature, vapor pressure deficit and shortwave radiation (vegetation sensitivity to climate) for 1984 - 2007. The spread in vegetation sensitivity has been normalized by the standard deviation of each histogram to allow for comparison on a single plot.

Row	Average	StandardDev	Area + (km^2)	Area - (km^2)	PointsPos	PointsNeg
NDVI v. Temp	0.68	2.95	27882880	7447892	7759	3186
NDVI v. VPD	3.66	10.11	25398868	9931904	6543	4402
NDVI v. Shortwave	-0.004	0.27	20738123	14731465	5860	5107

Table 3.1: Summary of global distribution of vegetation sensitivity.

displays a very broad distribution, nearly symmetric around zero (.004 %NDVI/(W/m^2)) (thin dotted line, Figure 3.1). Of the three climate variables for which we calculated the vegetation sensitivity, shortwave radiation has the smallest coefficient of variation (standard deviation/mean) for the majority of the globe, explaining the relatively small %NDVI change per W/m^2.

Going forward we will focus on the vegetation sensitivity to temperature. The geographical distribution of vegetation sensitivity shows a strong regional separation between positive and negative sensitivities (Figure 3.2A). Positive sensitivity is apparent across most of Europe, China, Northern Russia, The Amazon and African Rainforests. Negative sensitivity appears near regions of world primarily considered deserts; Southern and Eastern Africa, Australia, South West USA and Mexico, West India and the Caatinga region in the Northeast of Brazil. Generally the percent variance of annual NDVI explained by the temperature coincided strongly with the areas of strong vegetation sensitivity, with the percent variance explained mostly ranging from 25% in the highly sensitive areas to nearly 0% in other areas. In this case, areas with little sensitivity and low % variance explained are just as interesting as those areas that are highly sensitive.

3.2 Systematic Variation of Climate Constraint

To understand how vegetation sensitivity varies across global climate we split the climate into a series of percent bins (with equal number of observations in each) and calculated the area weighted mean vegetation sensitivity to temperature for all locations that fall within that bin. The mean vegetation sensitivities of each bin were mapped back to the globe

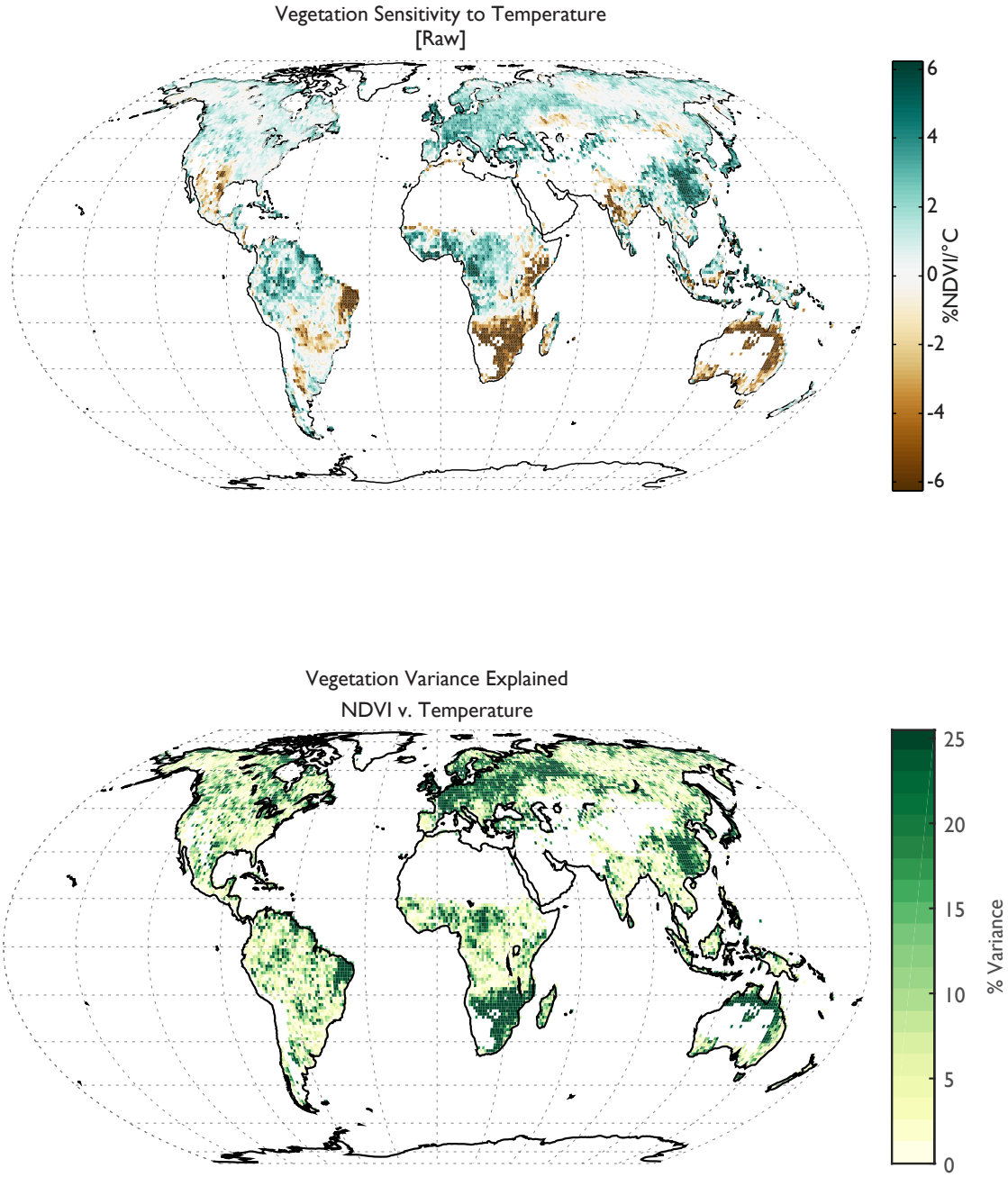

Figure 3.2: (A) The vegetation sensitivity to temperature. (B) The percent NDVI variance explained by the linear regression of Temperature.

to show the spatial distribution mean response in each climate. In particular we find a systematic variation in vegetation sensitivity across two climate variables, temperature and precipitation. First, the sensitivity of vegetation to temperature varies across places with different mean annual temperatures–e.g. the sensitivity of NDVI to temperature is positive and large in cold places and negative in hot places. Second, the sensitivity of vegetation simultaneously varies across precipitation –e.g. the sensitivity of NDVI to temperature becomes positive (too cold) when rainfall is larger than 1100 mm/year on average (Figure 3.7A). Vegetation sensitivity to temperature interacts with more than temperature, with the function changing as the balance of precipitation, shortwave radiation, vapor pressure deficit and temperature change from place to place.

3.3 Vegetation Constraint Varies across Temperature and Precipitation

Mean annual temperatures and precipitation have traditionally been used as the primary division between biome types [Whittaker 1970]. Here we look across two climate variables simultaneously to capture the variation of vegetation sensitivity to temperature. We expect precipitation (water supply) to help mitigate the high temperature heat stress plants experience through latent heat cooling from transpiration. Another way to visualize climatic constraints on vegetation that vary simultaneously in both temperature and precipitation space is to consider how the vegetation sensitivity to temperature varies from cold places to hot places for different rainfall rates. The transition from cold constrained regime (greener in warm years) to a warm constrained regime (browner in warm years) happens at places with higher average temperatures if they also have high precipitation levels. At places with lower rainfall (low rainfalls indicated by lighter blue temp in Fig. 3.4A), the transition from a cold constrained regime (green Figure 3.3B) to a warm constrained regime (brown Figure 3.3B) happens at places with cooler average temperature. The majority of grid cells in simultaneously warm (above 14 °C) and dry (below 1000 mm/year rainfall) conditions have negative vegetation sensitivity to temperature. At cooler temperatures the vegetation sensitivity is mostly positive (cold constrained) but without as pronounced a pattern across

rainfall (similar to the variation across temperature alone). At very high rainfall levels (beyond 3000 mm/year), even locations with high mean annual temperatures show positive sensitivity to temperature anomalies (greener when warmer). It is non-intuitive to call this very hot, very wet region cold constrained but this analysis shows that with large amounts of water available, warmer temperatures are still beneficial for increased greenness.

High annual rainfall allows for a positive sensitivity of vegetation to warmer years even at some of the hottest temperatures on vegetated land. When mapped spatially, by plotting the spatial points in each bin with the mean vegetation sensitivity, negative sensitivity to warming are primarily gathered around the edges of non-vegetated deserts of the North American Southwest, Sahel, South Africa and Australia as well as North East Brazil and the rain shadow of the Chilean Coastal Range (Figure 3.4B). For places with the highest mean rainfall (darkest blue line, Fig 3.4A, 1597 mm/year) there is no transition to too hot climate constraint at all, supporting the idea that if given sufficient water, plants still respond positively to increases in temperature.

When considering how vegetation responds to temperature across long-term mean temperature for all points, the sensitivity of vegetation to temperature switches from positive (cold constraint) to negative (warm constraint) at 16 °C (Figure 3.5A). As we also subdivide locations into groups based on mean precipitation, the general shape of the vegetation sensitivity lines across temperature space is very similar for different levels of rainfall, going from a strong cold constraint to a strong hot constraint at most levels of precipitation. However, the rainfall modulates the point where vegetation switches from cold constrained to warm constrained (where the constraint line crosses zero). The zero crossing point tends towards warmer values (14 °C to >21 °C) at higher rainfall rates (between 500mm/year and 1250 mm/year) with the highest rainfall category lacking a zero crossing and a too hot constraint altogether (Figure 3.4B). The exception is the lowest rainfall category (300 mm/year) which shows the opposite trend with the zero crossing point at a higher temperature (16 °C) compared to slightly wetter categories.

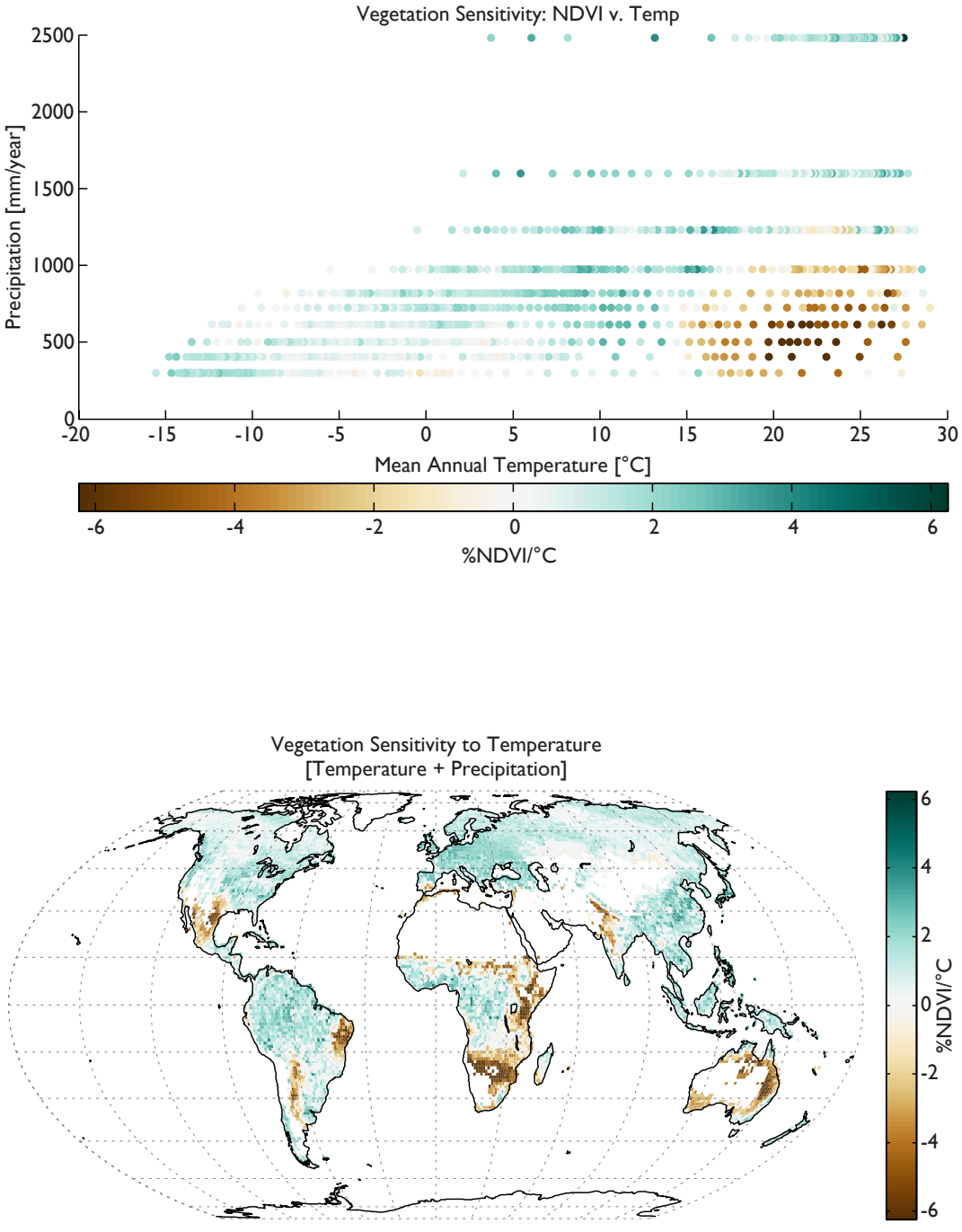

Figure 3.3: (A) The vegetation sensitivity binned in percentage bins in both Precipitation and Temperature to create a heat map of the means of the bins. (B) Temperature and Precipitation combined bins mapped to the globe.

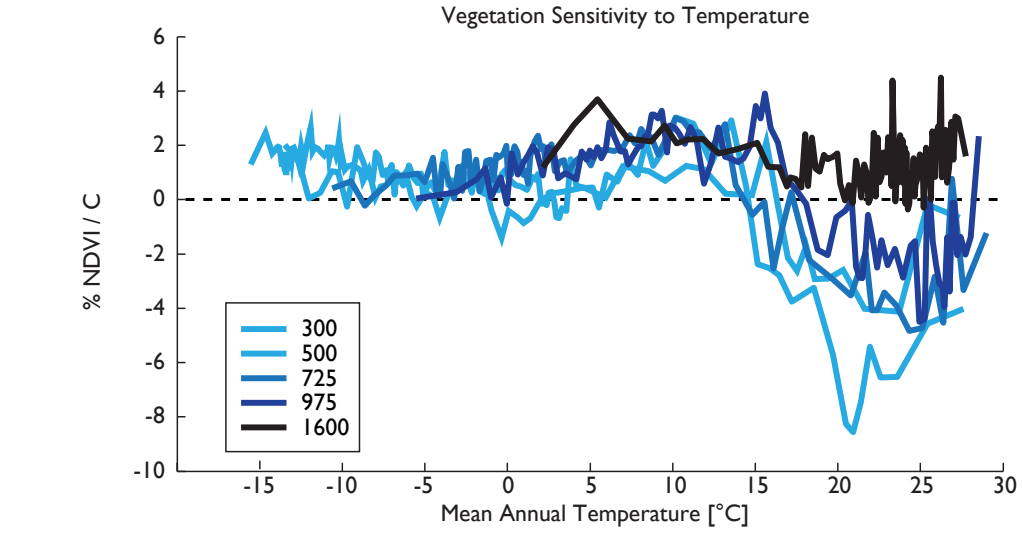

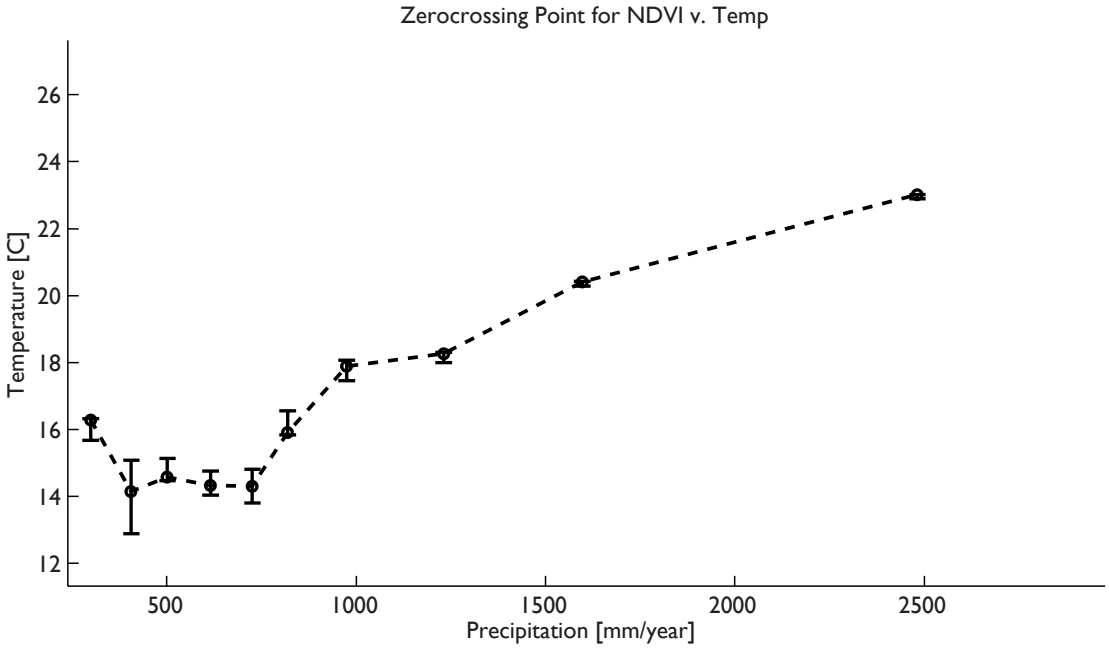

Figure 3.4: (A) Vegetation response to temperature binned across rainfall and temperature and plotted across temperature. (B) The temperature and precipitation at which the vegetation response to temperature crosses zero.

3.3.1 Vegetation sensitivity to Temperature

We will look first at the sensitivity of vegetation to temperature across places with different annual average temperatures (Figure 3.5). We find that in the coldest places on the globe, vegetation is constrained by cold, such that warmer years are also greener. The highest positive vegetation sensitivity to temperature occurs between 4 °C and 14 °C mean annual temperature, broadly including the Northern portion of the United States of America (US), major parts of Europe and the South Coast of China (Figure 3.5B). The absolute magnitude of vegetation sensitivity decreases from this point as we look to warmer parts of the globe until it crosses zero at approximately 16 °C. At places with mean annual temperatures hotter than this zero-crossing point the vegetation is less green when temperatures are higher (its "too hot") and can be considered constrained by high temperatures. These 'too hot' constrained areas include the South East of the US, most of Mexico, South East China and the southern portions of South America, Africa and Australia. As temperatures get even warmer the negative sensitivity of vegetation in 'too hot' regions returns towards zero, even going positive after approximately 23 °C. At very high rainfall levels, even locations with high mean annual temperatures show positive sensitivity to temperature anomalies (greener when warmer). Places with temperatures higher than 23 °C, include both the edges of deserts and tropical rainforest so that the average of a bin defined only along temperature shows vegetation to be weakly constrained by temperature on average, though it is actually a balance between strongly and weakly constrained places (see Figure 3.5B).

The systematic variation of vegetation sensitivity is not monotonic across places with different mean annual temperature and suggests that vegetation sensitivity to temperature is modulated by more than just the long-term temperature of a place. While the pattern of vegetation sensitivity across temperature space was positive in cold places and negative in hot places, when viewed across shortwave radiation space the response is much closer to monotonic (Figure 3.6A). The vegetation sensitivity across broad values of shortwave radiation starting with places that have low light levels all the way up to 190 W/m^2 (for reference,

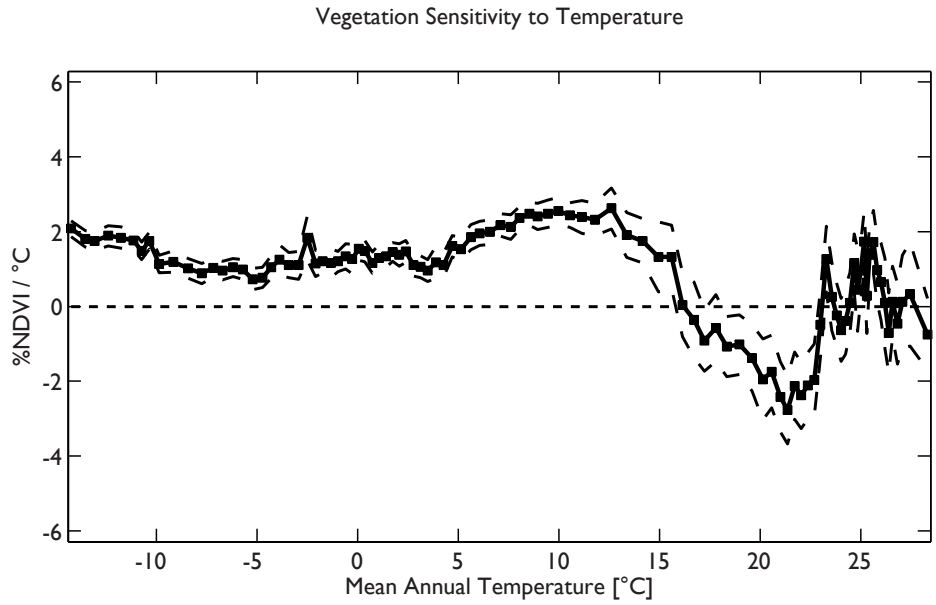

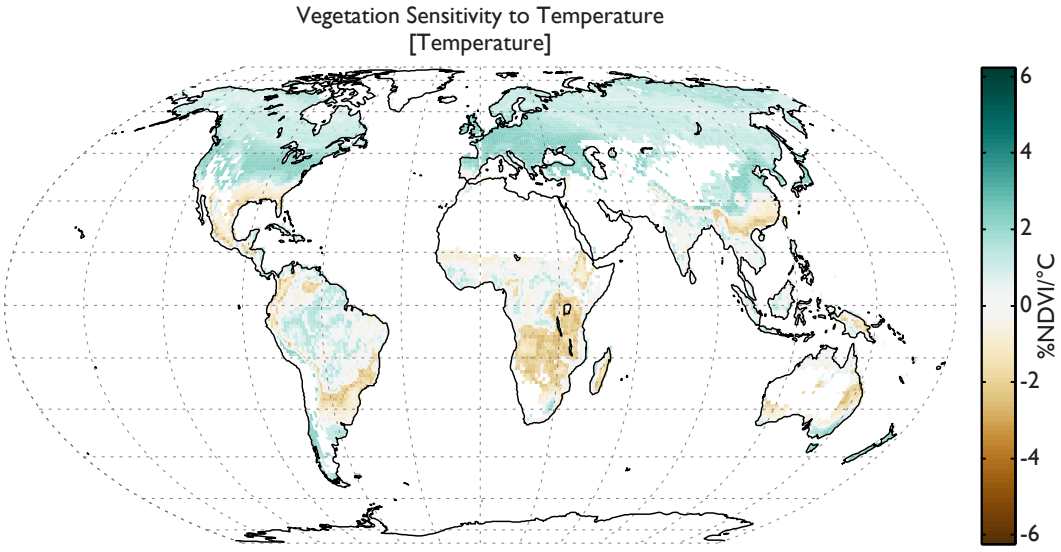

Figure 3.5: (A) The mean vegetation response binned along the long-term mean temperature. (B) The mean value of each bin is assigned to all the points of that bin to remap the mean vegetation response back to a map.

this is approximately the mean annual shortwave radiation of San Francisco, Managua and Madrid) show that vegetation is constrained by cold temperatures on average (greener in warmer years) (Figure 3.6). In places surface shortwave radiation values higher than 190 W/m2 the constraint linearly decreases until reaching zero at places with surface shortwave values of 210 W/m^2. In the brightest places (>210 W/m2), the sensitivity is negative (browner in warmer years). Unlike the variation in long-term temperature where vegetation sensitivity rebounds back to a weak constraint at high temperatures, the negative sensitivity of vegetation continues to get larger with increasing mean annual shortwave radiation up until the maximum of approximately 260 W/m^2. The areas of the strongest constraint by high temperatures (largest negative sensitivities) occur at very bright places–along the southern edge of the US South West deserts, the Sahara and the Australian deserts. Intermediate values of vegetation sensitivity highlight the edges of tropical forests, particularly the South American Savannah south of the Amazon Forest where there is a large area that transitions from nearly zero constraint towards a too hot constraint in the Caatinga region in the Northeast of Brazil. The systematic variation in the vegetation sensitivity to temperature across shortwave radiation shows that in addition to temperature itself, the mean incident energy is a factor in how sensitive the vegetation is to variations in temperature.

We expect there to be a systematic variation in the high temperature constraints on vegetation across precipitation space because increased availability of water buffers against damaging maximum temperatures. Precipitation supplies water to the terrestrial system that is then transpired through the vegetation during photosynthesis. Under hot conditions with sufficient water supply vegetation is able to transpire at a high rate. This serves to cool the vegetation through the waters latent heat of vaporization offsetting the heating from the air temperature and insolation. In the relatively hot places of the world the vegetation sensitivity to temperature becomes increasingly positive (greener in warmer years) in places with large annual mean precipitation, leveling off after values reach approximately 2300 mm/year (Figure 3.7). In dry places with low levels of precipitation there are areas of negative vegetation sensitivity to temperature (browner in warmer years). When we plot the

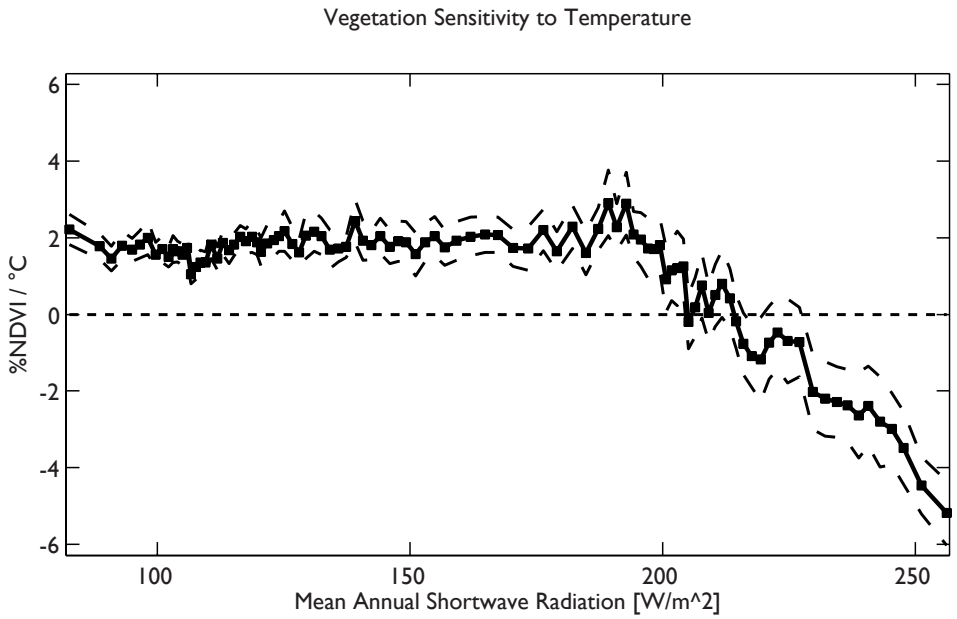

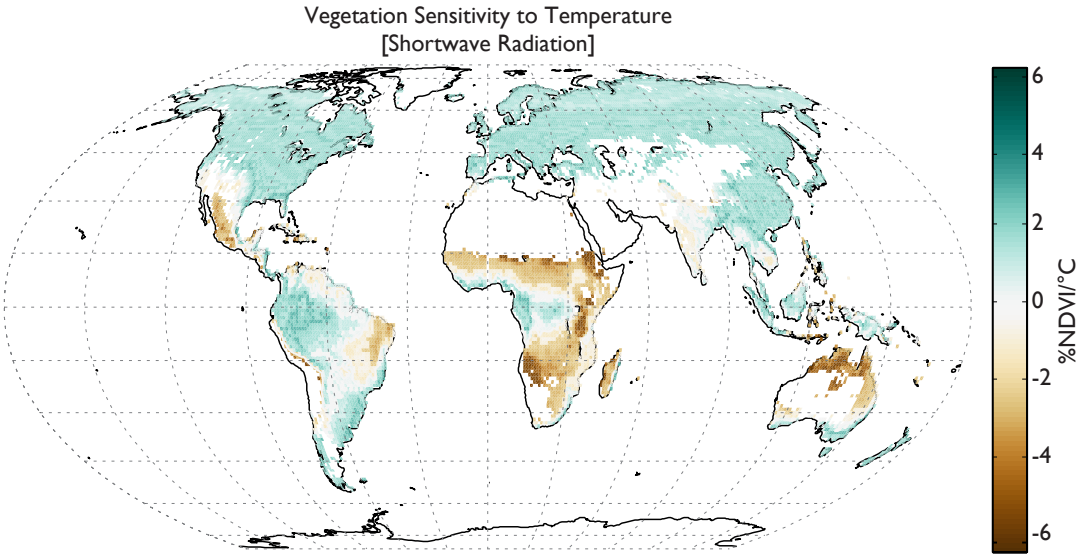

Figure 3.6: (A) The mean vegetation response binned along the long-term mean shortwave radiation. (B) The mean value of each bin is assigned to all the points of that bin to remap the mean vegetation response back to a map.

sensitivity of vegetation to temperature across precipitation space on a map, areas of high rainfall such as the tropics, South East North America and Pacific Northwest show up as having the biggest sensitivity to temperature. The interiors of both the North American and Asian continents, as well South Africa shows the broadest pattern of negative sensitivity to temperature (greener in cooler years). Vapor pressure deficit combines information about both the temperature and water content of the atmosphere to estimate how far a parcel of air is from being saturated, capturing the demand for water from the atmosphere that the vegetation experiences. Increasing temperature increases vapor pressure deficit through an exponential relationship, while increasing humidity decreases vapor pressure deficit. High values of vapor pressure deficit are dry and hot, while lower values are cold and/or wet. The sensitivity of vegetation to temperature across vapor pressure deficit space has a similar shape to that across shortwave radiation space, though the edges of deserts and the South American savannah appear with even more contrast (Figure 3.8). The temperature constraint on vegetation is positive (too cold) up until a vapor pressure deficit of approximately 7.5 hPa after which it becomes negatively constrained (too hot).

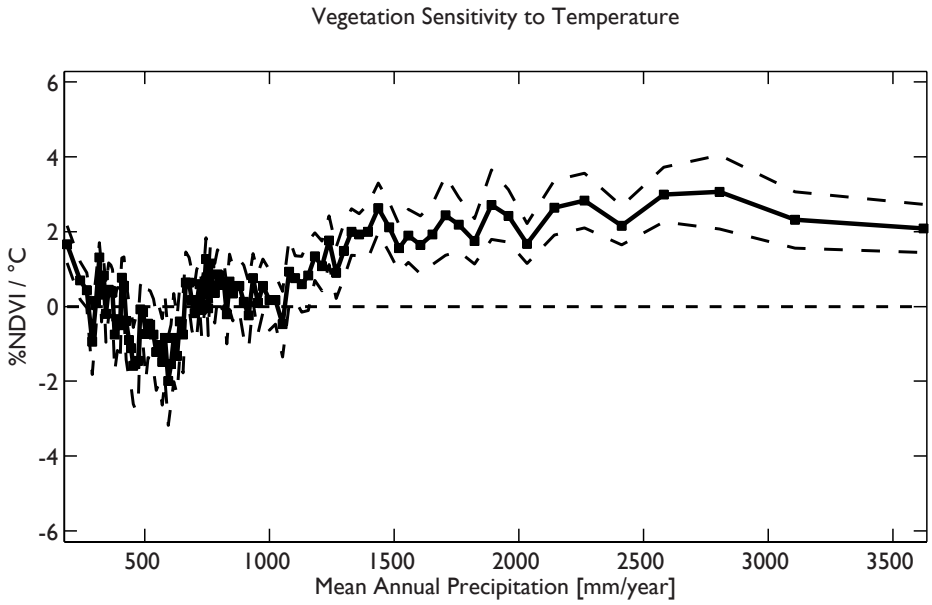

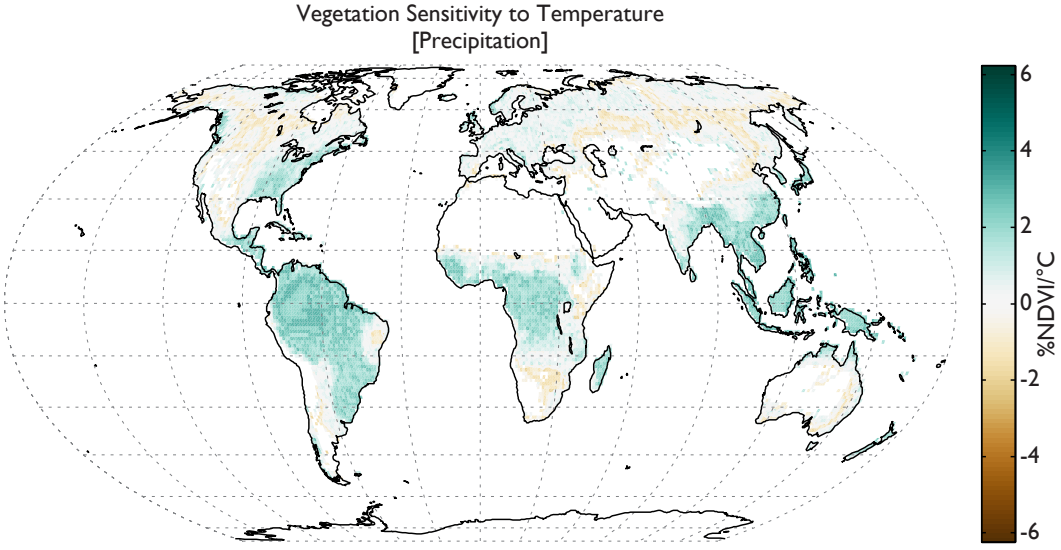

Figure 3.7: This figure uses the long-term mean Precipitation from 2001 2011. (A) The mean vegetation response binned along the long-term mean precipitation. (B) The mean value of each bin is assigned to all the points of that bin to remap the mean vegetation response back to a map.

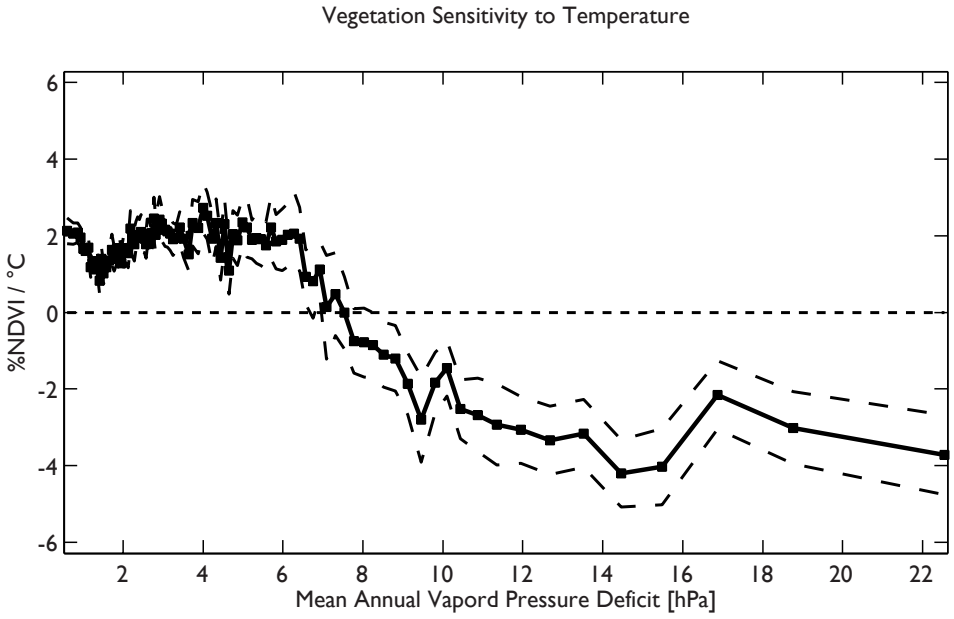

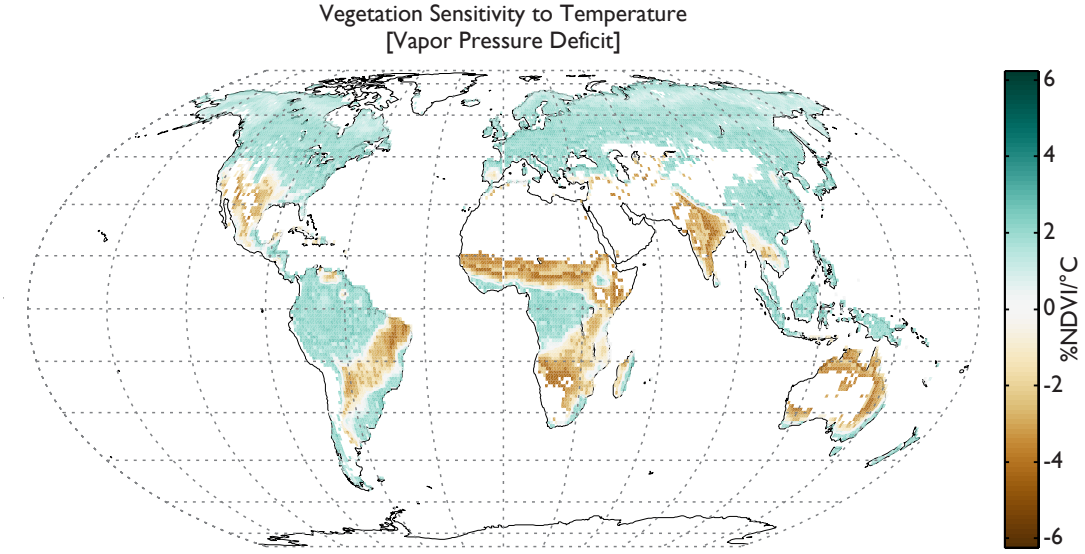

Figure 3.8: (A) The mean vegetation response binned along the long-term mean vapor pressure deficit. (B) The mean value of each bin is assigned to all the points of that bin to remap the mean vegetation response back to a map.

Chapter 4

DISCUSSION

Our analysis of vegetation sensitivity to temperatureusing NDVI provides an empirical map of climate constraints on vegetation. The global coverage and persistence of the NDVI time series, combined with global measurements of climate allows us to quantify the mean annual temperature of the onset of a too hot climate constraint and how the increased availability of water pushes this onset to a warmer temperature. Here we will discuss [1] the physiological mechanisms that link the inter-annual vegetation sensitivity to temperature with average annual conditions of precipitation and temperature, [2] how our data-driven analysis relates to previous climate classification approaches and efforts to model the climate constraints on vegetation. [3] We will discuss how this analysis can be used to constrain Earth System Models and the implications of our quantified climate constraints for predictions of vegetation change under a warming climate. [4] Finally, we will include a discussion of the limitations and interpretation of this analysis.

4.1 Distribution of Vegetation Sensitivity Across the Globe

The vegetation sensitivity to temperaturefor all points across the globe have distributions peaked near zero (Figure 3.1). However, it is the distribution of temperature sensitivity that has a mean value greater than zero for the globe. This excess of places constrained by cold temperatures is a result of the fact that the primary locations for too hot constrained vegetation are in limited dry areas around deserts (Figure 3.3). Although the major deserts of the world have been removed from our analysis, the vegetated edges are constrained by high temperatures and a lack of water for cooling.

Though the variation of sensitivity to each of these three climate variables is unique

across climate space, many of the patterns and interpretations hold true for the vegetation sensitivity to temperature. For the following discussion we will focus on the vegetation sensitivity to temperature.

4.2 Negative Ecosystem Sensitivity Shifted to Higher Temperatures by Increased Water Supply

Vegetation sensitivity to temperature does not trend monotonically from high positive sensitivity in cold places, to high negative response in the hot tropics. Although vegetation in cold locations does generally get greener in warmer years, at medium temperatures between 15C and 23C the sensitivity is negative (implying browning during warm years) and then rebounds to a neutral or even positive response (greener in hot years) at higher temperatures (Figure 3.5A). This recovery from negative to positive sensitivity at high temperatures correlates with an increase in mean rainfall and is confined to the wet tropics where there is heavy rain. Transpiration of water through stomata is tied directly to photosynthesis, as water is released while stomata are open to absorb atmospheric CO_2 to turn into sugars. The flux of water through stomata serves as coolant for the vegetation through the latent heat absorbed during the conversion from liquid water to gas. [Schlesinger and Jasechko 2014] [Jasechko et al. 2013]. If leaves get too hot, the proteins necessary for photosynthesis and plant growth are impeded and become less efficient [Eaton-Rye et al. 2011]. From our analysis we find that a greater supply of water (as indicated by higher rates of precipitation) can push the negative sensitivity of vegetation to temperature up by 9 degrees °C, and remove it entirely at the highest precipitation levels (greater than 2500 mm/year) [Figure 3.4B]. Locations of both low and high temperature show positive vegetation sensitivity to temperature suggesting that different mechanisms apply in the two different climate regimes. In very cold locations, the positive vegetation sensitivity to a warm year reflects either a positive response to increases in growing season temperature or an expansion of the growing season. Indeed, much of the NDVI variance in cold areas is concentrated in transition months at each end of the growing season. At locations with average temperatures below 14 °C vegetation sensitivity to

temperature shows little variation across precipitation values (different lines, Figure 3.4A), except at the driest locations on Earth (less than 500mm/year). In hotter locations, the limitation from temperature on vegetation differs across a gradient of water availability as represented by annual precipitation. We interpret this difference in temperatures sensitivity in different precipitation regimes as a coupling between the canopy temperature and the ability of leaves to regulate stomatal conductance during transpiration. Without considering both the precipitation and temperature of a location when evaluating the amplitude of vegetation sensitivity cause by climate we would not predict the correct distribution of vegetation sensitivity of temperature. This is particularly true at warmer locations but also plays a role in cold locations where we might intuitively expect a homogeneous positive sensitivity to temperature. However, the global pattern of vegetation sensitivity generated solely from the binned temperature (Figure 3.5B) fails to capture very dry cold areas in Northern Alaska and Siberia that have very low vegetation sensitivities to temperature because they area also very dry (Figure 3.3B). In a warming climate these cold places may not respond to the warming in an intuitive way because of the balance with water availability.

4.3 Comparison with Biome and Model Based Studies

Our work is not the first to address the determination of global vegetation distribution by climate, or try and determine the processes that constrains vegetation across the climate space. The work of climate classification [Peel et al. 2007] [Kottek et al. 2006] capture the distribution of current vegetation and the modeling of climate resource constraints [Churkina and Running 1998] [Nemani et al. 2003] illustrate our knowledge of climate constraints on vegetation. Our work expands on climate classification by using empirical vegetation sensitivity to gain inference into the physiological process that established and maintains the biome boundaries. Many features we observe from our calculations of vegetation sensitivity match well with these classic approaches. For example, the vegetation sensitivity to temperature binned (Figure 3.3B) captures an area of negative vegetation sensitivity to temperature along the southern boundary of the Sahara that correlates with area classified

as arid summer dry summer hot by Koppen-Geiger. The measured positive vegetation sensitivity captures the lack of cold constraint in the tropics. This positive vegetation sensitivity to temperature compares well to [Nemani et al. 2003] considering it is likely due to strong correlation with the limiting incident shortwave radiation [Supplement]. Our work is the first to quantify these vegetation climate sensitivities with an approach wholly dependent on data allowing for the processes of vegetation-climate interaction to be tested. The weak and negative vegetation sensitivity in Northern Alaska agrees with maps of climate constraint developed from outputs of Net Primary Productivity (NPP) from BIOMBGC [Churkina and Running 1998]. These modeling efforts capture many of the processes we see but, as they are based on the models themselves, would not serve to test the models. The constraint curves from BIOMEBGC allow insight into the aggregated response of that model, and given the good match with our observed metrics suggest that the model captures many of the processes that emerge from the data. The data necessarily contains more cross-correlations between climatic factors but the general shape of response found in the models supports the interpretations of vegetation sensitivity to temperature reflecting a combination of temperature and water processes at warmer temperatures.

4.4 Accounting for Effects of Temperature and Water on the Global Scale

There is a significant systematic variation of vegetation sensitivity to temperature across the climatic range of temperature, incident energy, water supply and water demand. We have quantified the mean response of ecosystems adapted to the climate states by binning the vegetation-temperature response across temperature, shortwave radiation, precipitation, and vapor pressure deficit. Our analysis provides functional forms for vegetation sensitivity to temperature in relation to global climate. This analysis can be used to constrain our near term predictions of vegetation response to global warming as well as the models used for long term predictions. Counter to a 'cold gets greener with warming' intuition, cold areas are also modulated by dryness, even across parts of the high latitudes we see a very weak sensitivity to temperature (little change in greenness with changes in temperature) that would

suggest little vegetation response to global warming in the near term. Bioclimatic envelope approaches would identify more productive regions expanding with warming temperatures, and consistently these high latitude regions are predicted to show gains in productivity in a warming climate [Soja et al. 2007].

However, from our analysis gains in productivity driven by warming alone do not seem likely unless water availability is also increased. As a second example, at this large scale we observe an approximately .2% increase in NDVI per degree Celsius widespread across the South American, African and Indonesian tropics (Figure 3.3 B). On a plant scale, experiments on individual species suggest that there is ultimately an upper temperature limit on vegetation [Battisti and Naylor 2009], fueling concern for the hot and highly productive tropical regions, along with the people they support. The positive temperature sensitivity of these warm wet ecosystems suggests that they may actually benefit from near term warming on the scale of inter-annual variations of temperature, able to buffer against damaging maximum temperatures with their access to water.

4.5 Interpretation of Vegetation sensitivity to Mean Annual Variables

4.5.1 NDVI as metric of vegetation sensitivity

We are interpreting the inter-annual vegetation sensitivity to climate using remotely sensed NDVI to represent the vegetation response. NDVI serves as a metric of greenness or chloroplast density, it has also been related to Leaf Area Index and Photosynthetically Available Radiation [Myneni et al. 2002]. From these relationships we consider the signal from NDVI as primarily related to the leaves of vegetation and their potential to fix sunlight into sugars. We assume here that the greening of an ecosystem signals that it is advantageous for the plants to deploy more chloroplast in an attempt to fix more carbon. While, on annual basis, an increase in greenness is a good metric for a positive vegetation sensitivity to climate that correlates with increased NPP [Myneni et al. 1995], it has been proposed that observed greening (from a closely related satellite metric) during the 2005 drought over the Amazon may

have resulted not from an increase in productivity, or even leaf area, but from an increase in leaf greenness due to drought deciduous trees dropping their leaves and later producing new leaves that were anomalously young for the time of year, and therefore greener [Huete et al. 2006]. We do not expect this effect to play a large role across the globe or alter our interpretation of the dominant sensitivity of vegetation to climate.

4.5.2 Limitations of using Mean Annual Quantities

In our analysis we focus on using mean annual values for greenness (from NDVI) and climate variables to capture information about the total productivity of a place. An increase in mean annual NDVI from one year to the next combines two potentially independent signals of changes in greenness 1) the increase in the maximum greenness and 2) an increase in the duration of the greenest season. Combining these two effects allow an equitable treatment of the globe, although the inter-annual variations is reflective of different months depending on location [Supplement]. Additionally, the standard 15-day composites available for NDVI observations add uncertainty in regards to the duration of the growing season as phenology can change on the order of days. By using mean annual values we capture the combination of both the amplitude of vegetation change and the potential change in duration. With nearly zero variance during non-vegetated months the mean annual values of NDVI are driven nearly exclusively by changes in the vegetation rather than changes in snow and soil moisture [Trishchenko et al. 2002].

Using the mean annual values of climate variables (i.e. temperature) in our analysis combines information about the monthly variance and phasing between climate variables. At the plant scale the ecosystem is in actuality responding to the environment on a timescale of minutes by regulating its response to the environment for maximum performance. An ecosystem that experiences large seasonality in precipitation that is strongly out of phase with insolation and temperature (i.e. wet winters, dry summers) will not respond to a change in the annual average precipitation the same way as an ecosystem with more broadly distributed climate (i.e. one with rainfall distributed throughout the year). Thus an increase

in rain during an already wet portion of the year (raising the mean annual value) would cause a different response than an increase in rain during a dry portion of the year. Although these sub-yearly time scale constraints on vegetation are of interest, we chose to use the mean annual values here for three reasons. First, it is expected that the mean annual climate is of first order importance in defining the systematic variance of temperature constraint on vegetation. Second, the mean annual values treat all global latitudes equitably, without prior knowledge of different seasonal cycles. Third, we can compare our results with previous efforts of climate classification, where mean annual climate was primarily used as thresholds. We propose investigation of the influence of seasonal cycles on the sensitivity of vegetation as a future direction for this research.

BIBLIOGRAPHY

Robert F. Adler, George J. Huffman, Alfred Chang, Ralph Ferraro, Ping-Ping Xie, John Janowiak, Bruno Rudolf, Udo Schneider, Scott Curtis, David Bolvin, Arnold Gruber, Joel Susskind, Philip Arkin, and Eric Nelkin. The version-2 global precipitation climatology project (GPCP) monthly precipitation analysis (1979present). *J. Hydrometeor*, 4(6):1147–1167, December 2003. ISSN 1525-755X. doi: 10.1175/1525-7541(2003)004¡1147:TVGPCP¿2.0.CO;2. URL http://dx.doi.org/10.1175/1525-7541(2003)004<1147:TVGPCP>2.0.CO;2.

Gregory P. Asner, Alan R. Townsend, and Bobby H. Braswell. Satellite observation of el nio effects on amazon forest phenology and productivity. *Geophys. Res. Lett.*, 27(7):981–984, April 2000. ISSN 1944-8007. doi: 10.1029/1999GL011113. URL http://dx.doi.org/10.1029/1999GL011113.

J.Timothy Ball, IanE. Woodrow, and JosephA. Berry. A model predicting stomatal conductance and its contribution to the control of photosynthesis under different environmental conditions. In J. Biggins, editor, *Progress in Photosynthesis Research*, pages 221–224. Springer Netherlands, January 1987. ISBN 978-94-017-0521-9. URL http://dx.doi.org/10.1007/978-94-017-0519-6$_4$8.

David. S. Battisti and Rosamond L. Naylor. Historical warnings of future food insecurity with unprecedented seasonal heat. *Science*, 323 (5911):240–244, January 2009. doi: 10.1126/science.1164363. URL http://www.sciencemag.org/content/323/5911/240.abstract.

CLINE BOISVENUE and STEVEN W. RUNNING. Impacts of climate change on natural forest productivity evidence since the middle of the 20th century. *Global Change Biology*,

12(5):862–882, May 2006. ISSN 1365-2486. doi: 10.1111/j.1365-2486.2006.01134.x. URL http://dx.doi.org/10.1111/j.1365-2486.2006.01134.x.

Baozhang Chen, Guang Xu, Nicholas C. Coops, Philippe Ciais, John L. Innes, Guangyu Wang, Ranga B. Myneni, Tongli Wang, Judi Krzyzanowski, Qinglin Li, Lin Cao, and Ying Liu. Changes in vegetation photosynthetic activity trends across the asia-apacific region over the last three decades. *Remote Sensing of Environment*, 144 (0):28–41, March 2014. ISSN 0034-4257. doi: 10.1016/j.rse.2013.12.018. URL http://www.sciencedirect.com/science/article/pii/S0034425714000030.

Galina Churkina and Steven W. Running. Contrasting climatic controls on the estimated productivity of global terrestrial biomes. *Ecosystems*, 1(2):206–215, March 1998. ISSN 1432-9840. doi: 10.1007/s100219900016. URL http://dx.doi.org/10.1007/s100219900016.

D. P. Dee, S. M. Uppala, A. J. Simmons, P. Berrisford, P. Poli, S. Kobayashi, U. Andrae, M. A. Balmaseda, G. Balsamo, P. Bauer, P. Bechtold, A. C. M. Beljaars, L. van de Berg, J. Bidlot, N. Bormann, C. Delsol, R. Dragani, M. Fuentes, A. J. Geer, L. Haimberger, S. B. Healy, H. Hersbach, E. V. Hlm, L. Isaksen, P. Kllberg, M. Khler, M. Matricardi, A. P. McNally, B. M. Monge-Sanz, J.-J. Morcrette, B.-K. Park, C. Peubey, P. de Rosnay, C. Tavolato, J.-N. Thpaut, and F. Vitart. The ERA-interim reanalysis: configuration and performance of the data assimilation system. *Q.J.R. Meteorol. Soc.*, 137(656):553–597, April 2011. ISSN 1477-870X. doi: 10.1002/qj.828. URL http://dx.doi.org/10.1002/qj.828.

Curtis A. Deutsch, Joshua J. Tewksbury, Raymond B. Huey, Kimberly S. Sheldon, Cameron K. Ghalambor, David C. Haak, and Paul R. Martin. Impacts of climate warming on terrestrial ectotherms across latitude. *Proceedings of the National Academy of Sciences*, 105(18):6668–6672, May 2008. doi: 10.1073/pnas.0709472105. URL http://www.pnas.org/content/105/18/6668.abstract.

G. A. Duff, B. A. Myers, R. J. Williams, D. Eamus, A. O'Grady, and I. R. Fordyce. Seasonal

patterns in soil moisture, vapour pressure deficit, tree canopy cover and pre-dawn water potential in a northern australian savanna. *Aust. J. Bot.*, 45(2):211–224, January 1997. URL http://www.publish.csiro.au/paper/BT96018.

Julian J Eaton-Rye, Baishnab C Tripathy, and Thomas D Sharkey. *Photosynthesis: plastid biology, energy conversion and carbon assimilation*, volume 34. Springer Science & Business Media, 2011. ISBN 940071579X.

P. Friedlingstein, P. Cox, R. Betts, L. Bopp, W. von Bloh, V. Brovkin, P. Cadule, S. Doney, M. Eby, I. Fung, G. Bala, J. John, C. Jones, F. Joos, T. Kato, M. Kawamiya, W. Knorr, K. Lindsay, H. D. Matthews, T. Raddatz, P. Rayner, C. Reick, E. Roeckner, K.-G. Schnitzler, R. Schnur, K. Strassmann, A. J. Weaver, C. Yoshikawa, and N. Zeng. Climate-carbon cycle feedback analysis: Results from the c4mip model intercomparison. *J. Climate*, 19(14):3337–3353, July 2006. ISSN 0894-8755. doi: 10.1175/JCLI3800.1. URL http://dx.doi.org/10.1175/JCLI3800.1.

Bardan Ghimire, Christopher A Williams, Jeffrey Masek, Feng Gao, Zhuosen Wang, Crystal Schaaf, and Tao He. Global albedo change and radiative cooling from anthropogenic land-cover change, 1700 to 2005 based on MODIS, land-use harmonization, radiative kernels and reanalysis. *Geophys. Res. Lett.*, page 2014GL061671, October 2014. ISSN 1944-8007. doi: 10.1002/2014GL061671. URL http://dx.doi.org/10.1002/2014GL061671.

Samuel N. Goward, Brian Markham, Dennis G. Dye, Wayne Dulaney, and Jingli Yang. Normalized difference vegetation index measurements from the advanced very high resolution radiometer. *Remote Sensing of Environment*, 35(23):257–277, February 1991. ISSN 0034-4257. doi: 10.1016/0034-4257(91)90017-Z. URL http://www.sciencedirect.com/science/article/pii/003442579190017Z.

BRENT N. HOLBEN. Characteristics of maximum-value composite images from temporal AVHRR data. *International Journal of Remote Sensing*, 7(11):1417–

1434, November 1986. ISSN 0143-1161. doi: 10.1080/01431168608948945. URL http://dx.doi.org/10.1080/01431168608948945.

Alfredo R Huete, Kamel Didan, Yosio E Shimabukuro, Piyachat Ratana, Scott R Saleska, Lucy R Hutyra, Wenze Yang, Ramakrishna R Nemani, and Ranga Myneni. Amazon rainforests greenup with sunlight in dry season. *Geophysical Research Letters*, 33(6), 2006. ISSN 1944-8007.

Raymond B Huey. Physiological consequences of habitat selection. *American Naturalist*, pages S91–S115, 1991. ISSN 0003-0147.

Scott Jasechko, Zachary D. Sharp, John J. Gibson, S. Jean Birks, Yi Yi, and Peter J. Fawcett. Terrestrial water fluxes dominated by transpiration. *Nature*, 496(7445):347–350, April 2013. ISSN 0028-0836. URL http://dx.doi.org/10.1038/nature11983.

William M. Jolly, Ramakrishna Nemani, and Steven W. Running. A generalized, bioclimatic index to predict foliar phenology in response to climate. *Global Change Biology*, 11 (4):619–632, April 2005. ISSN 1365-2486. doi: 10.1111/j.1365-2486.2005.00930.x. URL http://dx.doi.org/10.1111/j.1365-2486.2005.00930.x.

Markus Kottek, Jrgen Grieser, Christoph Beck, Bruno Rudolf, and Franz Rubel. World map of the koppen-geiger climate classification updated. *Meteorologische Zeitschrift*, 15 (3):259–264, 2006. ISSN 0941-2948.

Marc J. Metzger, Robert G. H. Bunce, Rob H. G. Jongman, Roger Sayre, Antonio Trabucco, and Robert Zomer. A high-resolution bioclimate map of the world: a unifying framework for global biodiversity research and monitoring. *Global Ecology and Biogeography*, 22(5):630–638, May 2013. ISSN 1466-8238. doi: 10.1111/geb.12022. URL http://dx.doi.org/10.1111/geb.12022.

R.B. Myneni, F.G. Hall, P.J. Sellers, and A.L. Marshak. The interpretation of spectral

vegetation indexes. *Geoscience and Remote Sensing, IEEE Transactions on*, 33(2):481–486, March 1995. ISSN 0196-2892. doi: 10.1109/36.377948.

R.B Myneni, S Hoffman, Y Knyazikhin, J.L Privette, J Glassy, Y Tian, Y Wang, X Song, Y Zhang, G.R Smith, A Lotsch, M Friedl, J.T Morisette, P Votava, R.R Nemani, and S.W Running. Global products of vegetation leaf area and fraction absorbed PAR from year one of MODIS data. *Remote Sensing of Environment*, 83(12):214–231, November 2002. ISSN 0034-4257. doi: 10.1016/S0034-4257(02)00074-3. URL http://www.sciencedirect.com/science/article/pii/S0034425702000743.

R. R. Nemani, C. D. Keeling, H. Hashimoto, W. M. Jolly, S. C. Piper, C. J. Tucker, R. B. Myneni, and S. W. Running. Climate-driven increases in global terrestrial net primary production from 1982 to 1999. *Science*, 300(5625):1560–1563, 2003.

Keith W Oleson, David M Lawrence, B Gordon, Mark G Flanner, Erik Kluzek, J Peter, Samuel Levis, Sean C Swenson, E Thornton, and Johannes Feddema. Technical description of version 4.0 of the community land model (CLM). 2010.

M. C. Peel, B. L. Finlayson, and T. A. McMahon. Updated world map of the kppen-geiger climate classification. *Hydrol. Earth Syst. Sci. Discuss.*, 4(2): 439–473, March 2007. ISSN 1812-2116. doi: 10.5194/hessd-4-439-2007. URL http://www.hydrol-earth-syst-sci-discuss.net/4/439/2007/.

Jorge E. Pinzon and Compton J. Tucker. A non-stationary 19812012 AVHRR NDVI3g time series. *Remote Sensing*, 6(8):6929–6960, 2014. ISSN 2072-4292. doi: 10.3390/rs6086929. URL http://www.mdpi.com/2072-4292/6/8/6929.

Steven W. Running, Ramakrishna R. Nemani, Faith Ann Heinsch, Maosheng Zhao, Matt Reeves, and Hirofumi Hashimoto. A continuous satellite-derived measure of global terrestrial primary production. *BioScience*, 54(6):547–560,

June 2004. doi: 10.1641/0006-3568(2004)054[0547:ACSMOG]2.0.CO;2. URL http://bioscience.oxfordjournals.org/content/54/6/547.abstract.

William H. Schlesinger and Scott Jasechko. Transpiration in the global water cycle. *Agricultural and Forest Meteorology*, 189190(0):115–117, June 2014. ISSN 0168-1923. doi: 10.1016/j.agrformet.2014.01.011. URL http://www.sciencedirect.com/science/article/pii/S0168192314000203.

G. Louis Smith, Anne C. Wilber, Shashi K. Gupta, and Paul W. Stackhouse. Surface radiation budget and climate classification. *J. Climate*, 15(10):1175–1188, May 2002. ISSN 0894-8755. doi: 10.1175/1520-0442(2002)015¡1175:SRBACC¿2.0.CO;2. URL http://dx.doi.org/10.1175/1520-0442(2002)015<1175:SRBACC>2.0.CO;2.

Amber J. Soja, Nadezda M. Tchebakova, Nancy H.F. French, Michael D. Flannigan, Herman H. Shugart, Brian J. Stocks, Anatoly I. Sukhinin, E.I. Parfenova, F. Stuart Chapin III, and Paul W. Stackhouse Jr. Climate-induced boreal forest change: Predictions versus current observations. *Global and Planetary Change*, 56(34):274–296, April 2007. ISSN 0921-8181. doi: 10.1016/j.gloplacha.2006.07.028. URL http://www.sciencedirect.com/science/article/pii/S0921818106001883.

Charles Warren Thornthwaite. An approach toward a rational classification of climate. *Geographical review*, 38(1):55–94, 1948. ISSN 0016-7428.

Alexander P Trishchenko, Josef Cihlar, and Zhanqing Li. Effects of spectral response function on surface reflectance and NDVI measured with moderate resolution satellite sensors. *Remote Sensing of Environment*, 81(1):1–18, July 2002. ISSN 0034-4257. doi: 10.1016/S0034-4257(01)00328-5. URL http://www.sciencedirect.com/science/article/pii/S0034425701003285.

Robert Harding Whittaker. Communities and ecosystems. *Communities and ecosystems.*, 1970.

Guang Xu, Huifang Zhang, Baozhang Chen, Hairong Zhang, John L Innes, Guangyu Wang, Jianwu Yan, Yonghong Zheng, Zaichun Zhu, and Ranga B Myneni. Changes in vegetation growth dynamics and relations with climate over chinas landmass from 1982 to 2011. *Remote Sensing*, 6(4):3263–3283, 2014.

L. Zhou, R. K. Kaufmann, Y. Tian, R. B. Myneni, and C. J. Tucker. Relation between interannual variations in satellite measures of northern forest greenness and climate between 1982 and 1999. *J. Geophys. Res.*, 108(D1):4004, January 2003. ISSN 2156-2202. doi: 10.1029/2002JD002510. URL `http://dx.doi.org/10.1029/2002JD002510`.

Liming Zhou, Compton J. Tucker, Robert K. Kaufmann, Daniel Slayback, Nikolay V. Shabanov, and Ranga B. Myneni. Variations in northern vegetation activity inferred from satellite data of vegetation index during 1981 to 1999. *J. Geophys. Res.*, 106(D17): 20069–20083, September 2001. ISSN 2156-2202. doi: 10.1029/2000JD000115. URL `http://dx.doi.org/10.1029/2000JD000115`.